

Two to Tango: Hybrid Light and Backscatter Networks for Next Billion Devices

Ander Galisteo*
IMDEA Networks
Universidad Carlos III de Madrid
Madrid, Spain
ander.galisteo@imdea.org

Ambuj Varshney*
Uppsala University
Uppsala, Sweden
ambuj.varshney@it.uu.se

Domenico Giustiniano
IMDEA Networks
Madrid, Spain
domenico.giustiniano@imdea.org

ABSTRACT

The growth rate of Internet-of-Things (IoT) devices sold globally is constantly lower than the forecast. This deceleration is caused in part by the need for batteries and the scalability cost for their replacement. Backscatter has attracted significant interest over the past couple of years to enable sustainable sensing devices by eliminating batteries. IoT devices have been designed for transmitting sensed data with backscatter, but the question of efficient reception of data with battery-free devices is still open. As shown in this paper, classical low-power Radio Frequency (RF) envelope detectors are affected by low sensitivity, false detection alarms, and low energy efficiency. We argue that Light Fidelity (LiFi) can provide downlink and harvesting medium as LED lights are becoming pervasively deployed for illumination. We show, for the first time, that the advantages of LiFi and RF backscatter can be combined for battery-free communication. We design a low-power platform that leverages the complementary nature of these two mediums. We demonstrate that our platform removes energy-inefficiency in the downlink reception typical of RF backscatter, and significantly expands the deployment scenarios for battery-free tags when compared to conventional single-technology designs.

CCS CONCEPTS

• **Computer systems organization** → **Sensor networks**; • **Hardware** → *Networking hardware; Sensor devices and platforms; Wireless devices.*

ACM Reference Format:

Ander Galisteo, Ambuj Varshney, and Domenico Giustiniano. 2020. Two to Tango: Hybrid Light and Backscatter Networks for Next Billion Devices. In *The 18th Annual International Conference on Mobile Systems, Applications, and Services (MobiSys '20)*, June 15–19, 2020, Toronto, ON, Canada. ACM, New York, NY, USA, 14 pages. <https://doi.org/10.1145/3386901.3388918>

1 INTRODUCTION

Internet-of-Things (IoT) devices are entering into our life. However, all forecasts in terms of number of sold IoT devices are constantly

*Both authors contributed equally to this work.

Permission to make digital or hard copies of all or part of this work for personal or classroom use is granted without fee provided that copies are not made or distributed for profit or commercial advantage and that copies bear this notice and the full citation on the first page. Copyrights for components of this work owned by others than ACM must be honored. Abstracting with credit is permitted. To copy otherwise, or republish, to post on servers or to redistribute to lists, requires prior specific permission and/or a fee. Request permissions from permissions@acm.org.

MobiSys '20, June 15–19, 2020, Toronto, ON, Canada

© 2020 Association for Computing Machinery.

ACM ISBN 978-1-4503-7954-0/20/06...\$15.00

<https://doi.org/10.1145/3386901.3388918>

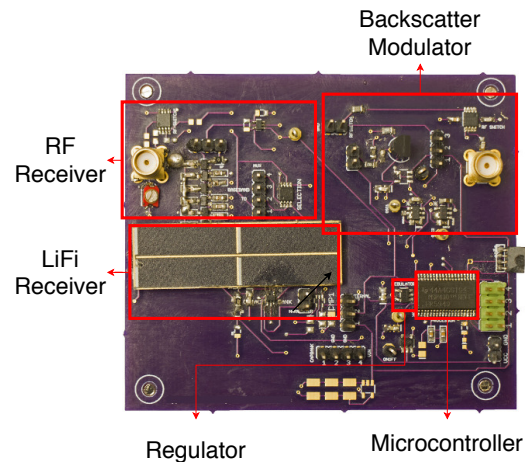


Figure 1: Battery-free LiFi and RF-Backscatter tag. The tag operates on the energy harvested from ambient light. It supports uplink using RF-backscatter, and downlink using a small solar cell-based LiFi/RF receiver.

below the expectations [40]. In 2012, IBM predicted a total of 1 trillion IoT devices sold by 2015. In 2017, Cisco predicted 50 billion devices by 2020. In 2018, GSMA predicted 25 billion devices by 2025. But, in 2018 there have been 7 billion connected IoT devices [6]. Most likely, the *need for batteries* is playing a tremendous role in this deceleration. Scalability issues caused by the replacement of batteries, the limited sensor functionality caused by the physical dimension of batteries, and the environmental harm of battery disposal [7, 50] make IoT systems heavily dependent on batteries to operate.

While battery-free devices that operate on harvested energy have long been touted as a panacea [30, 37, 48, 49, 56, 60] fundamental roadblocks impede this vision. In particular, the lack of sufficiently powerful energy harvesting sources forces the battery-free devices to work under extreme energy constraints. In fact, battery-free devices largely rely on Radio Frequency (RF)-based energy sources, but the RF energy harvesting works at a much shorter range than communication [18]. The limited amount of harvested energy means that battery-free devices operate under extreme energy constraints and need to sacrifice functionality and efficiency to achieve continuous operation. As shown in this work, this, in turn, leads to low wireless performance across several dimensions including low spectral efficiency, uni-directional communication, and low receiver sensitivity. For instance, existing work primarily uses backscatter for communication from the battery-free device, but they are inefficient when downlink communication is needed. We propose a different approach, where we leverage the

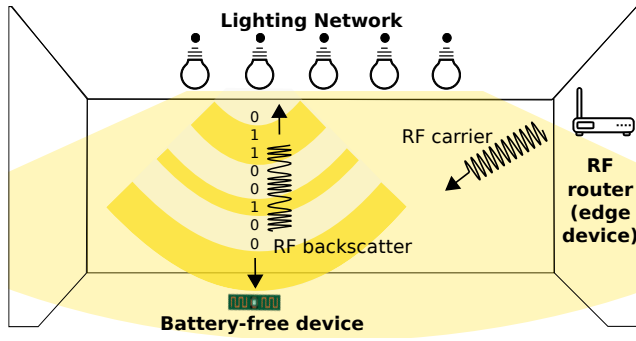


Figure 2: High-level view of the system. EDISON can make use of the existing infrastructure, which includes smart bulbs and RF router in order to support battery-free devices.

complementary properties of modulated light and radio for passive communication. An example of our system is shown in Fig. 1.

Light fixtures densification. Dense lighting networks are emerging due to technology push driven by the need for providing uniform illumination for user comfort. In our view, this also provides an opportunity to design dense networks that harvest energy for battery-free devices with orders of magnitude better performance. There will be no need anymore to stay close to the RF source to harvest enough energy. Light bulbs are becoming also modulated to transmit data through Visible Light Communication (VLC), and networking solutions are commonly referred as LiFi (Light Fidelity) systems. This opens the opportunity to communicate and harvest through light. But visible light is not always better than radios – light suffers in non-line-of-sight and uplink transmissions [29, 64]. We find that LiFi and RF backscatter are individually incomplete.

LiFi and RF bottleneck. LiFi is an efficient downlink communication and energy delivery mechanism. However, LiFi devices encounter challenges with supporting uplink capabilities. Uplink transmissions achieved through LiFi are prohibitively energy expensive and can disturb the uniform illumination of the room. On the other hand, RF-backscatter is an efficient transmission mechanism and enables low-power wireless transmissions at orders of magnitude lower energy cost compared to conventional radios [27, 57, 65]. However, RF-backscatter devices suffer from challenges in reception due to limitations of the receiver employed on these devices, i.e., an envelope detector. We present these challenges in Section 2.

Vision for the deployment. We tackle several challenges related to these mediums and demonstrate that, in fact, these are complementary mediums, and design a system that we call EDISON. A high-level illustration of the envisioned deployment is presented in Fig. 2. LED bulbs will be uniformly deployed for uniform illumination. In the same environment, we expect that the RF router that provides Internet connection will operate as edge device for passive communication. LED bulbs and RF router will be retrofitted with realistic changes, yet large potential to enable our passive communication system. Going beyond the transceiver circuitry required by LiFi technology, LED bulbs will require an RF receiver operating in the frequency of interest. Intelligent light bulbs from major vendors already provide similar functionalities, for instance, to control the hue and brightness of the bulb itself. Our bulbs transmit LiFi data to the battery-free device and receive their

RF data. RF carrier generator for backscatter is outsourced to the RF router, which can use current WiFi chipsets for this operation. In a real deployment, the role of RF and LiFi may change, and it might be beneficial to receive or harvest energy using RF carrier instead of LiFi. We discuss such scenarios in Section 7.1.

We envision our system to enable application scenarios such as greenhouses and smart-houses (Section 7.3). These environments provide conditions suitable for our system, which at present may be constrained due to limitations of LiFi or RF-backscatter as modality. We take a step forward into enabling these applications through our battery-free design.

Main contribution. We present the design and quantitative assessment of EDISON, a bi-directional and passive communication system that operates under overall consumption smaller than of conventional RF designs. EDISON integrates LiFi and RF for passive communication. The key technical contributions are the following:

- This is the first paper that demonstrates that LiFi downlink and RF backscatter uplink solve several bottlenecks of these technologies when taken in isolation;
- Our tag is the first to integrate capabilities to harvest and receive with solar cells in passive communication systems;
- We propose a low-power processing mechanism of symbols with a microcontroller (MCU) triggered only by wake-up mechanisms and low-power timers;
- We make other contributions, such as investigating the usage of the LiFi transmitter as oscillator for RF backscatter.

Our experiments demonstrate that our system allows continuous reception of LiFi data without any battery up to 250 bit/sec.

2 CHALLENGES

In this section, we discuss challenges in using LiFi and RF technologies on battery-free sensor platforms.

2.1 LiFi Bottlenecks

The problem in using LiFi systems comes from the high power consumption for receptions and transmissions, which limits the use on battery-free platforms. This is caused by the following bottlenecks:

- **B1:** LiFi front-ends employed in state-of-the-art systems highly depend on power-hungry amplifiers to amplify the weak signals received by photodiodes;
- **B2:** LiFi uses intensity modulation for transmission. However, sampling of light intensity for reception is energy expensive. Current low-power solutions remove sampling mechanisms but still consume significant energy;
- **B3:** uplink transmission with LED or retroreflected light is power-hungry and/or cause disturbance to user comfort.

We discuss these issues in detail in what follows. In order to address **B1** and **B2**, we need a new design that is more energy efficient in the whole chain of LiFi data reception. For **B3**, we explore the usage of RF backscatter as alternative solution (Section 3).

LiFi Front-end. LiFi front-ends employed in state-of-the-art systems are energy expensive consuming few-to-tens of milliwatts of power for their operation [31, 54]. A high power consumption restricts the operation of such receivers on the energy harvested from the ambient environment, which is commonly several orders

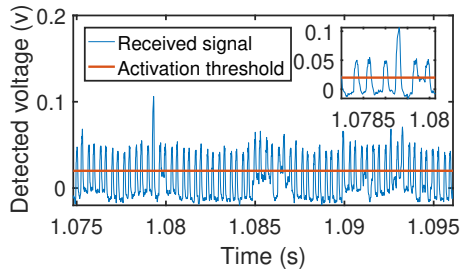


Figure 3: False triggers. Output signal from the RF envelope detector at 868 MHz. We see significant channel activity due to ambient wireless traffic. The top right corner of the graph shows a magnified section of the graph.

of magnitude lower. The reason for the high power consumption is the use of photodiodes for their operation. Photodiodes have a good responsivity but are fundamentally characterized by the small reception area. As such, they always need energy-expensive trans-impedance amplifiers to amplify the weak signals received.

Recent works such as RetroVLC [29] and PassiveVLC [64] design LiFi receivers increase the circuitry complexity in the analog domain to reduce the power-hungry processing in the digital domain. However, they still rely on photodiodes and energy-expensive trans-impedance amplifiers in the analog domain.

Data acquisition. Most existing LiFi systems employ a direct detection method to receive and process LiFi data [20]. It consists of sampling the light intensity periodically using an analog-to-digital converter (ADC) and interpreting the received bits to recover the data. Periodic sampling with the ADC requires continuous operation of expensive energy timers and frequent waking up of the microcontroller. Current low-power solutions for communication [29, 64] and sensing [59, 60] remove sampling mechanisms and introduce a comparator. Visible light-sensing mechanisms operate at a much lower frequency rate. Moreover, designs for data communication are dependent on access to timing information, which depletes the scarce harvested energy.

Uplink transmissions. Generating light for uplink transmissions is energy expensive. A VLC transmitter typically relies on LEDs for transmission. However, even ultra-low-power LEDs consume energy in the order of 50-80 mW for transmission. Similarly, a conventional radio transceiver is hugely energy expensive to operate within the constraints of the harvested energy [27].

RetroVLC and PassiveVLC demonstrate uplink by reflecting light. Their tags backscatter the light they receive. As impinging light from LEDs in the ceiling is in the visible spectrum, reflected light covers the visible spectrum as well. This brings practical issues: the illumination of these tags can be distracting in a living environment, they require larger tag size due to the need of LCD shutters for modulating the light, and increase their uplink range at the cost of high directionality and reduced communication reliability.

2.2 Backscatter Downlink Bottleneck

Ultra-low-power tags use simple receivers such as passive envelope detectors as opposed to IQ receivers [34]. This causes the following major bottlenecks:

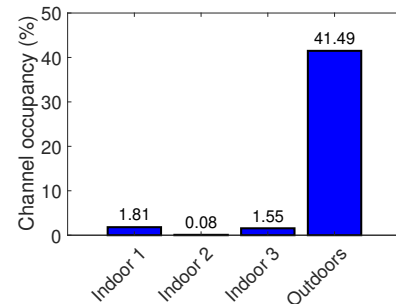


Figure 4: Channel occupancy. We experimented at different locations within our campus (indoors and outdoors), and observed significant channel occupancy due to ambient traffic.

- **B4:** passive RF receivers are affected by false detections, as any ambient traffic within the frequency band would trigger simple envelope detectors;
- **B5:** the sensitivity of an energy-efficient passive receiver is very low, in the order of -30 dBm [44]. This also limits the amount of RF energy that can be harvested.

We discuss **B4** and **B5** in detail in this section to motivate our choice for downlink LiFi (Section 3).

Ambient traffic. In recent years, wireless sensors and other wireless applications have seen significant growth. This has increased the Cross-Technology Interference (CTI) significantly. While in traditional active communication systems CTI mainly causes packet losses, CTI is particularly challenging in battery-free platforms. A constant CTI level is beneficial for battery-free devices as energy could be harvested for the operation of the tag. Nevertheless, any changes in the CTI level is problematic, as it triggers the envelope detectors commonly employed for receptions on these platforms. The precious harvested energy collected over a significant period is served to process false wake-up events.

We experimentally study this problem and observe that the trend towards large scale deployments of low-power wide-area network standards such as LoRa negatively affects our envelope detectors. To demonstrate this phenomenon, we perform an experiment where we collect energy measurements using a zero consumption envelope detector and a logic analyzer at four different locations of our campus and city, three indoor in different locations and heights on the same building and one outdoors in front of our university campus. We calculate the wake-up events encountered in these experiments. Without powering the tag, we measure the output of the envelope detector at each location for three minutes.

An example of the collected results can be seen in Fig. 3. In our experience, we have found that the comparator of our design may be triggered with voltage changes as low as 20 mV [41]. A low detection threshold improves the sensitivity of the RF receivers, but also causes them detect the communication of other devices. In turn, this may trigger the MCU causing an undesired increase in the consumption of the tag as well as errors in the communication. We quantify this problem by measuring the percentage of channel occupancy time caused by CTI. In Fig. 4, we can see that the occupancy can already reach over 40%.

Density of Carrier Emitter. Battery-free devices mostly rely on RF-based energy sources, but the RF energy harvesting works at a much shorter range than communication. In fact, tags need to

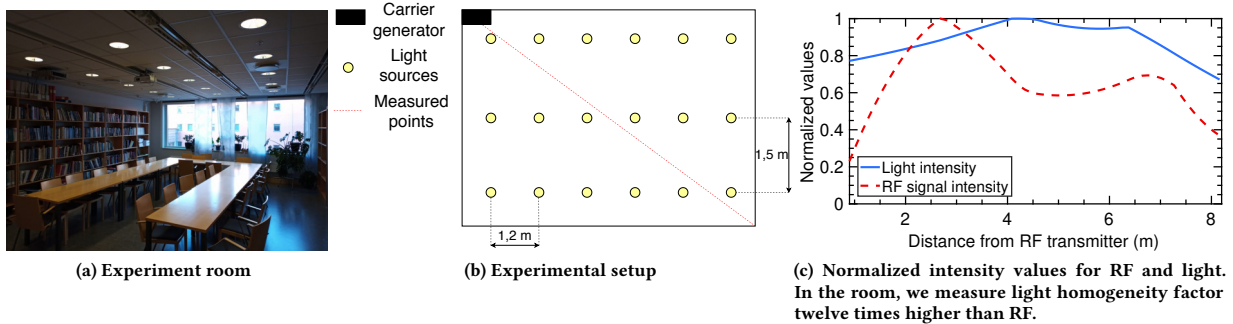


Figure 5: Homogeneity comparison between light and RF carrier signal. In a typical indoor environment, we find that the light is significantly more homogeneous compared to RF signals.

harvest a minimum amount of energy to turn on (*harvesting threshold*). A tag typically needs a few tens of μW to turn on and begin operation [45]; hence the range is usually limited by whether such energy can be obtained from the harvesting source. This presents a scalability challenge: we need dense deployments of high-power RF emitters for ubiquitous harvesting. While dense RFID deployments have been touted as a solution, technology trends do not suggest this as a viable solution, and facts show that there are only isolated deployments such as industrial IoT (e.g. supply chain warehouses).

We instead expect a typical indoor deployment to have a single device such as a WiFi router that provides the necessary carrier signal to support downlink communication. However, such a scenario limits the operational range to proximity to the carrier emitter device due to the RF effects mentioned above. In order to quantify this problem, we place a carrier generator, which is a USRP Ettus B200 at the corner of the room, an ideal location for a WiFi router in a home, and we program it to generate a signal with a maximum strength of 17 dBm. Next, we observe the signal strength of the carrier signal across the room using an RF spectrum analyzer as a receiver together with the light intensity measured with a luxmeter. We measure the uniformity of RF and light strength samples at different 2D positions inside the room. The values of RF and light signal’s intensities have been normalized and plotted across the diagonal of the room. We show the experiment room and setup in Fig. 5a and Fig. 5b, respectively, showing the room’s dimensions.

The results are displayed in Fig. 5c. We observe that close to the RF emitter, contrary to our expectation, the RF signal intensity is weaker because we are close to the wall and a metallic stand, which might have impacted the signal. However, overall, it can be seen that the RF signal has a large peak to average ratios.

Key takeaways. Here we present the most important lessons learned from the challenges and results presented in this section:

- LiFi systems suffer from challenges of energy-efficient reception and limited uplink capabilities.
- RF backscatter tags are challenged due to the capabilities of the envelope detector. We find that high channel occupancy leads to false triggers due to ambient wireless traffic.
- Light conditions in the indoor environment are more uniform and homogeneous when compared to RF carrier signal.

3 EDISON

We advocate a design that uses LiFi downlink and RF backscatter uplink. Our solution is called EDISON. We design the system with the objective of being able to communicate using hybrid RF-light medium while having a very low-power consumption to support the operation on the harvested energy.

In Section 3.1, we first show that LiFi downlink offers the opportunity to solve the bottlenecks in backscatter downlink, and then explore our main design choices to address the LiFi bottlenecks. The main components of our system are then presented in Section 3.2, and the details of the main components are then presented in Section 3.3.

3.1 Design principles

Light infrastructure is getting denser at a higher pace than RF infrastructure, and RF alone is not deployed so pervasively. This has consequences on the intensity level measured with RF and light. To illustrate this point, in the same setting as for the RF experiments conducted in Fig. 5c, we also measure the light levels using a sensor tag light meter. The room uses standard light fixtures for illumination. As for RF, we collect light strength at different locations in the room and plot the normalized values across the diagonal of the room. The results are displayed in Fig. 5c. We measure light homogeneity factor twelve times higher than RF (0.502 versus 0.040). Our experiments have been performed in a relatively old office environment. We expect that new rooms will have a factor of illuminance uniformity above 0.6 [14]. In conclusion, dense deployments of LED bulbs allows to address bottleneck **B5** and provide denser infrastructural elements for energy harvesting.

Downlink LiFi addresses bottleneck **B4**. First, in indoor environments with uniform lighting, any changes in ambient light caused by human activity will cause infrequent changes in a small area, avoiding to trigger the low-power receiver if unnecessary. Second, human activity such as walking, which can disturb the ambient light environment, occurs at a much slower rate when compared to traffic from ambient signals. Finally, because of the directionality of LiFi downlink, LiFi receivers are also significantly less sensitive to changes caused by other LiFi communication in the area.

In order to solve bottleneck **B1**, we propose to leverage solar cells both to harvest energy and receive LiFi data at very low power.

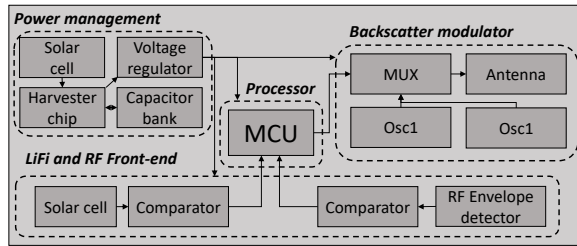


Figure 6: Overview of EDISON tag. It can be divided into four functional blocks; a microcontroller which runs the baseband processing logic, a power management unit, LiFi/RF receiver to support downlink communication, and a RF backscatter modulator for uplink transmissions.

RF backscatter provides a solution to **B3**, but it requires careful design of the elements in the system and their interaction. Our approach to addressing **B2** is finally presented in Section 4.

3.2 Overview

In this section, we provide an overview of our system and describe the three major components of our system.

Tag. The tag is the key component of the system. It harvests energy from the ambient light using solar cell and stores this energy on a small capacitor using a harvester circuit. The tag uses this energy to power a low-power microcontroller, the VLC receiver, the RF envelope detector and the backscatter transmitter. While operating on this harvested energy, the tag does baseband processing to receive transmissions using light, and can also transmit messages such as uplink transmissions using RF backscatter mechanism.

LED bulb. LiFi bulbs jointly provide the energy required by the tag to operate and downlink communication data. We also integrate an RF-transceiver in the bulb to support reception of backscatter messages. We note that most smart LED bulbs already have radio transceivers integrated and we might require minimal changes in the hardware to support the reception of RF backscatter signals.

Edge Device. The final component of our system is an edge device that is responsible for coordinating the downlink transmissions from the LiFi Transmitter. Further, the edge device is also equipped with a carrier generating device to provide necessary external carrier signal to enable uplink transmissions through the backscatter mechanism.

3.3 Tag

In this section, we discuss the design of the tag. We provide a high-level overview of the tag in the Fig. 6. It consists of four main components - LiFi front-end, backscatter modulator, a power management unit, and a processor. We present the first three components in this section, while the baseband processing logic and processor is presented in Section 4.

3.3.1 LiFi Front-end.

Instead of power-hungry amplifiers and photodiodes (bottleneck **B1**), in our system, we have a solar panel operating in photovoltaic mode. This allows having a zero power consumption for the LiFi front-end in our tags. Solar cells have larger reception areas than photodiodes. This is an advantage for harvesting but reduces the response time with respect to photodiodes. However, this does not

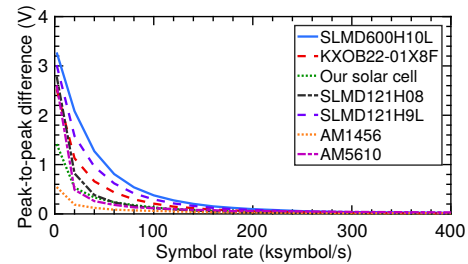


Figure 7: Performance of commercially-available solar cells. Distinguishing between the ON and OFF states of a LiFi transmitter becomes difficult at higher symbol rates since the peak-to-peak voltage difference becomes small.

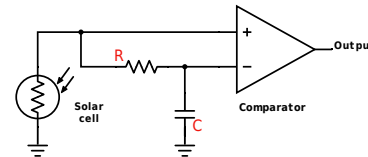


Figure 8: LiFi receiver schematic. A solar cell coupled with a thresholding circuit enables LiFi reception at sub- μ W of power consumption

impact us, as the baseband processing on low-power microcontroller limits our ability to support high bitrate transmissions.

Selecting solar cells. We evaluate the responsiveness to changes in light levels of several existing solar cells. As a transmitter device, we use a controllable LED connected to a pulse-wave generator that creates an alternating sequence of 1s (LED on) and 0s (LED off). We test seven solar cells with a form factor suitable for wearable applications. Five of these are monocrystalline with different dimensions and parameters, while two are amorphous silicon cells. We connect all solar cells to the ADC of a logic analyzer to find the peak-to-peak difference in the signal amplitude.

Fig. 7 demonstrates that all seven solar cells have similar patterns. As the sending symbol rate increases, the solar cells' ability to distinguish between the two LED states diminishes. We choose the SLMD121H04L [23] (< \$6) cell for our tag. This solar cell allows us to detect transmissions at a frequency as high as 180 ksymbol/s. It is also small and generates high short-circuit currents.

Digitizing solar cell output. The output of the solar cell is an analog signal representing the light conditions. This needs to be digitalized, and on active LiFi receivers, this step is performed using an analog to digital (ADC) converter.

We overcome this challenge by building on recent low-power visible light systems that have used a comparator coupled with a low pass filter as thresholding circuit for communication [29, 64] and sensing [59, 60]. We build on these designs and demonstrate it can enable downlink LiFi communication even while receiving communication data with the solar cell. The schematic is illustrated in Fig. 8. Fig. 9 compares the energy efficiency of our receiver to conventional radio transceivers and also to a LiFi receiver implemented using transimpedance amplifier. We are orders of magnitude more energy-efficient when compared to these designs.

3.3.2 Backscatter Modulator.

To support up-link transmissions, we use the backscatter mechanism. Backscatter enables transmissions at significantly lower

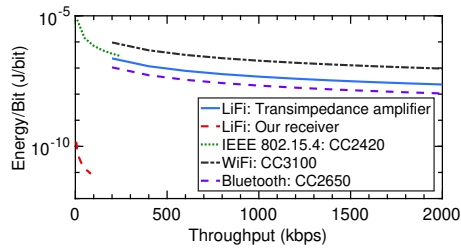


Figure 9: LiFi receiver comparison. Energy consumption/throughput comparison among LiFi receivers and modern RF chips. The ultra-low power receiver meets its performance goals of large energy saving while providing a sufficient data rate for downlink passive communication.

energy cost compared to the conventional transceivers by reflecting or absorbing ambient wireless signals [34, 57].

The ability to harvest a small amount of energy with dense LED bulbs deployment can allow us to avoid relying purely on energy from the RF router for harvesting. We exploit this energy budget for performing RF backscatter with frequency shifting for increased RF communication range [27]. Using frequency shifting, the range of such a transmitter can be quite high; for example, recent work has shown that the backscattered signal can be received across several walls in a home [47, 57]. Thus, we do not need dense edge devices deployed as RF carrier generators, and we demonstrate in Sec. 5 that only one device per home (e.g., integrated in a WiFi router) can suffice for uplink.

At a high level, the modulator works using two low-power oscillators, that generates frequency representing the two symbols 0 and 1, generating FSK modulation similarly to [57]. We select these symbols depending on the payload to be transmitted using a low-power multiplexer chip. This signal is used to control the backscatter frontend, which reflects or absorbs the incident carrier signal. We can support operation both in the 868 MHz and the 2.4 GHz band, while consuming a peak power of 70 μ W and 650 μ W, respectively. Our bit-rate in this work has been restricted to 2.9 kbps building on LoRea [57]. However, LoRea also supports higher bit-rate without significantly increasing the energy cost at the expense of reduced range. The tag also integrates an RF envelope detector that consumes up to 20 μ W at a sensitivity of about -30 dBm.

LiFi as Oscillator. On tags, the generation of the clock signal using oscillators is essential and commonly the most energy-expensive operation [2, 65]. In the design of the EDISON tag, among the components used in the communication blocks, the oscillator consumes the most energy. Further, the energy consumption of the oscillator increases with the oscillating frequency. Commonly a significant frequency shift is required, as this influences the self-interference from the carrier signal [57]. However, this increases the power consumption of the oscillator.

Through LiFi as Oscillator, we explore eliminating oscillators from the design of the tag and delegating this necessary task to external infrastructure, the LiFi transmitter. Eliminating oscillators from the design of the tag can enable us to reduce the power consumption of the tag. This is because we may be able to configure the magnitude of frequency shifts through LiFi, and support schemes such as frequency division multiplexing [58].

At a high level, this mechanism works as follows. The LiFi transmitter modulates the light with the clock signal. This signal is received by the solar cell and results in corresponding changes in the output of the cell. As we had seen in Fig. 7, these changes could be seen across a diverse set of solar cells. Next, the analog changes are digitized using a comparator to square signal, which could be used as a clock source for the RF-backscatter baseband processing. In our tag, this signal could be used instead of the signal generated from the local oscillator. Overall the power consumption is dictated by the comparator and is within a few μ Ws. The use of LiFi as an oscillator does not restrict the modulation scheme.

3.3.3 Power Management.

Power management is a crucial operation of the tag due to the battery-free nature. Our tag harvest energy from ambient light, stores the energy onto a small capacitor, and provides it to the components on the board for their operation. The fluctuations in voltage due to change in the voltage of the capacitor is challenging for battery-free systems [12, 35]. We overcome this by using a low-power regulator and operate the entire board at a low-voltage of 2.2 V to minimize the power consumption.

4 PROTOCOL

Design of protocol to leverage the hybrid medium while operating under the constraints of the harvested energy is one of the contributions that we make in this paper. We design the protocol to achieve meagre power consumption which, as an example, in our experiments, even allows continuous reception of LiFi data without intermittent behavior typical to battery-free systems. We discuss the design of the protocol next.

4.1 Energy-efficient LiFi Reception

Most existing LiFi systems use energy-expensive mechanisms to perform the necessary baseband processing to receive LiFi transmissions [16]. This involves sensing the light signal using a photodiode coupled with a transimpedance amplifier. The light signal is digitized and processed using ADCs. However, this is a prohibitively expensive operation when operating on harvested energy as it requires continuously polling and processing from the MCU.

Recent low-power LiFi systems overcome this limitation by using an event-based mechanism [29, 64]. These systems react to an external event such as interrupts instead of periodically sampling the channel to detect changes in the light intensity levels. These interrupts are generated using low-power comparators, which, as we had discussed in Section 3.3.1, help us to avoid the energy-expensive ADCs. Our protocol also uses event-based design. We keep the energy-expensive MCU to be in a low-power state for a vast majority of the time. The MCU awakens only when there is an external event caused by changes in the light intensity levels. However, we overcome limitations of existing event-based LiFi receivers that perform significant processing to measure the symbol period. Instead of keeping track of time by involving the MCU to measure clock cycle count, our system simplifies this design by using a low-power timer. This allows to place the energy-expensive MCU to low-power state in between processing of the symbol.

At a high level, our LiFi receiver mechanism works as follows: We monitor the output of the comparator in the LiFi receiver. Next,

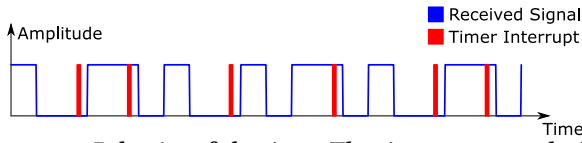


Figure 10: Behavior of the timer. The timer resets each time a rising or falling edge is found. If it triggers, it means that there is no edge between two symbols, and thus, two consecutive symbols with the same value have been received.

the change in the light level due to LiFi transmission causes the MCU to be woken out of the sleep state. MCU’s low-power timer is compared against the symbol period and interprets the incoming symbol. Finally, once the symbols are received, the MCU constructs the frame and processes the data.

To prevent flickering and support uniform illuminance during the downlink communication, we use Manchester coding. This ensures that even if data is transmitted, the LED bulb has a constant DC value of 50% of the high level of the signal. This encoding has another feature that we exploit: It ensures that irrespective of the content of the bitstream, the maximum consecutive symbols with the same value can be only two.

The reception logic operates as follows: As the tag switches on, it places the MCU to the low-power state to preserve the scarce harvested energy. Next, it waits for interrupts from the LiFi receiver’s comparator to receive ongoing LiFi transmission. Due to the inherent 1-bit nature of the comparator, we are limited to only the information about the transitions between high and low states. We precisely encode LiFi data within the timing information when the transition happens. This, however, requires us to maintain a notion of time at the tag which we achieve using a 32 kHz timer. This helps us consume a much lower power consumption to maintain time as compared to state-of-the-art works [29, 64] enabling us to sleep between the reception of symbols. A question we may ask is: *What should be the period of the timer event to aid in symbol detection?*

The duration of the timer has to be such that is between the symbol duration and twice the symbol duration. In order to avoid problems such as frequency offset of the oscillator, we set a conservative value of 1.5 times the symbol duration for the timer event. We illustrate the behavior in Fig. 10. From an implementation point of view, we detect symbols in the following way. We set the timer once the interrupt due to a rising or falling edge is found. Next, we distinguish if we have received a single symbol or contiguous symbols in the following way. If we receive the timer event before receiving an interrupt from the comparator, we know contiguous symbols have been received, and vice-versa. We end the transmission when we receive two continuous timer events without the comparator being triggered. This is because due to Manchester encoding, it is not possible to receive two symbols with similar value. An event with timer firing twice means that three contiguous symbols have been received, which cannot be possible unless transmission has concluded or there is an error which results in the case that we discard the LiFi frame.

We have two key advantage when using the aforementioned approach when compared to traditional sampling method: (i) There are hardly any synchronization related issues between transmitter and receiver which is common to sampling-based state-of-the-art

Preamble	SFD	Src. address	Dst. Address	Frame Length	Payload
32	16	8	8	32	0-MAX

Table 1: Frame structure and size (symbols)

Component	Name	Price (\$)
Solar Cell 6 cm ² (Receiver)	SLMD121H04L [23]	4,70
Energy Harvester (Power Management)	Texas Instruments BQ25570 [53]	3,13
Solar Cell 42.18 cm ² (Harvester)	MP3-37 [42]	4,77
Comparator (VLC/RF Receiver)	NCS2200 [41]	0,13
Microcontroller	MSP430FR5969 [52]	2,34
Oscillator (Backscatter Modulator)	Linear Technology LTC 6906 [33]	1,63
Multiplexer (Backscatter Modulator)	ADG904 multiplexer [5]	2,48
Regulator (Energy Management)	S-1313 [3]	0,32
RF Switch (Backscatter Modulator)	HMC190BMS8[4]	2,59
RF Envelope Detector (Receiver)	HSMS286C[11]	0,723
Backscatter Receiver	CC1310 [51]	34,22
VLC Transmitter (Platform)	BeagleBone Black [8]	63,75
Carrier Generator	B200 USRP [13]	888,16

Table 2: Main components used in the design of EDISON

LiFi systems, and (ii) Baseband processing is minimized due to timer-based events which helps to conserve scarce energy and maintain low power mode.

Frame structure. We show the frame structure in the Table 1. We store the received symbols into a circular memory structure. Our protocol detects a valid frame by comparing the preamble and Start Frame Delimiter (SFD). To support deployments with a dense number of tags, we also maintain space for TX and RX ID.

4.2 Backscatter Uplink

Our protocol also takes care of the uplink needed to have a bi-directional system. We achieve this using the backscatter mechanism. We implement the uplink baseband processing using timers similar to LiFi downlink logic. The timer generates interrupts at the symbol rate of uplink transmission. During these timer events, we select the oscillator that corresponds to the bit to be transmitted.

5 EVALUATION

We evaluate different aspects of our system. The highlights of the results presented in this section are as follows:

- We extensively evaluate EDISON in a range of conditions. Our experiment shows the ability to receive using LiFi up to 5 kbps and uplink transmissions using RF backscatter at 20 meters in NLOS conditions while operating battery-free on harvested energy.
- We demonstrate the ability to achieve continuous LiFi reception without duty cycling on the harvested energy at 250 bps under 500 Lux light. This is due to the low-power consumption of the LiFi receiver and baseband processing logic.
- EDISON introduces the concept of LiFi as an oscillator. This enables us to delegate the functionality of energy-expensive oscillator to the LiFi transmitter infrastructure. Our results demonstrate the ability to support a frequency as high as 90 kHz.

5.1 Experiments setup

EDISON has been designed with the components shown in Table 2. On the infrastructure’s side we use a BeagleBone Black (BBB) and the software and firmware of OpenVLC [15], transmitting LiFi data using On-Off keying (OOK) modulation. This translates to 1 bit every two symbols. We modulate the data to a GPIO. Then, we use an external driver to power up the voltage and connect it to a LED

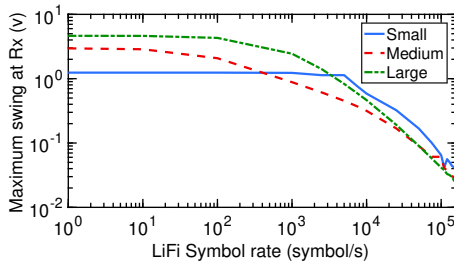


Figure 11: Solar cell voltage swing. We measure the maximum voltage swing at the output of the solar cell of different sizes. We see a larger size increases the capacitance. Capacitance effects reduce the swing at high symbol rates.

bulb of 4.3 W. The BBB is also connected to a Texas Instruments CC1310 that has been configured as a FSK receiver. This allows the bulb to directly control the handshake of communication with the tag. Both are connected through serial. Unless otherwise stated, we perform measurements at approx 500 lux, which is similar to levels commonly found in the indoor environment.

For the RF carrier generator, we use a B200 USRP generating a carrier at 868 MHz and transmitting with a power of 17 dBm. In the future, this element could also be designed and integrated with the edge device to minimize the cost of it. For instance, RF carrier generator at 2.4 GHz for backscatter could use current WiFi chipsets, that already support this operation.

Our tag harvests energy from a small credit card-sized solar cell (Powerfilm MP3-37 [42]), which is combined with an energy harvester circuit based on Texas Instruments BQ25570 [53]. The harvested energy is stored in a supercapacitor of up to few-mF in capacity. Next, as the charge on the capacitor varies due to the charging or discharging cycle, we use a low-power regulator (S-1313 [3]) to stabilize the voltage and keep it at a constant level. Once enough energy is harvested for the operation of the microcontroller MSP430FR5949 [52], it performs local processing, uplink transmissions or downlink receptions. To perform uplink transmission, we use the backscatter modulator designed using low-power oscillator LTC 6906 [33], ADG704 multiplexer [5], and HMC190BMS8 RF switch [4]. We perform downlink reception using a LiFi receiver or RF envelope detector depending on the experiment. The RF envelope detector is implemented using diode HSMS286C, which is also used in envelope detectors used in related systems. Further, we receive through LiFi using a solar cell SLMD121H04L [23]. We digitize the analog signal through a thresholding circuit designed using a comparator NCS2200 [41].

5.1.1 Cost.

In this section, we discuss the cost of designing the EDISON tag and LiFi transmitter. We note that, as we have designed only a few prototypes, the cost is significantly higher.

Tag. We list the cost of the components from a popular online store and show them in Table 2. The cost of PCB is 15 USD (excluding the cost of the components), which can be significantly lowered when done at scale. Overall, a single PCB, together with the components costs approx 38\$. The cost of components for an RF only version of the board would be 18.11\$, and a LiFi only would be 15.39\$. We note that the cost difference to integrate the LiFi receiver on a

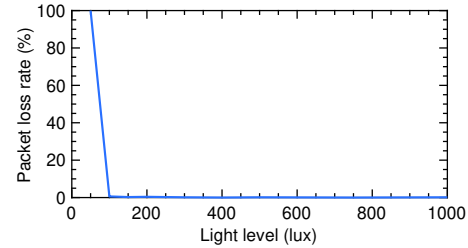


Figure 12: Packet loss rate and light levels. As we increase the light intensity levels, the packet loss rate decreases. At low light levels, we encounter high packet loss rate, as the light intensity is small to trigger the comparator.

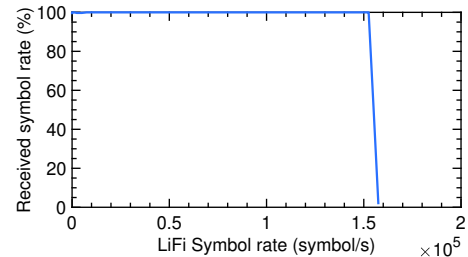


Figure 13: Received symbol rate and LiFi communication frequency. Increasing the LiFi communication frequency, causes the voltage swing to become progressively smaller. At 150 ksamples/s it is insufficient to trigger the comparator, thus preventing successful reception.

standard backscatter tag is nominal ($\approx 2.72\$$) when compared to the advantages gained in functionality.

LiFi Transmitter. The cost of the used LED is 3\$, and the Beagle-Blone Black we use is 64\$. The OpenVLC platform is a versatile research board and its code could be ported in the future into other embedded platforms to significantly lower the cost.

Next, we evaluate our system in a range of conditions that applications might encounter.

5.2 Data acquisition

Our LiFi front-end has two key components, the solar cell and the comparator. We measure the swing (difference between high and low symbols) obtained at different transmission rates for 3 different solar cells. The sizes are between the ones found in Table 2. The swing is necessary for the comparator to be triggered.

The results are presented in Fig. 11. At low frequencies, no matter the size, the solar cell is able to fully transition. This means that bigger areas can collect more energy and thus, show bigger swings. Nevertheless, the solar cells have capacitance effects that increase with the reception area. The capacitance limits its frequency response. In Fig. 11, we observe that, at higher frequencies, smaller solar cells show better behavior for communication as they transit faster. For the rest of the experiments with solar cells, we will use the smallest one, as its behavior is the best at high frequencies.

Fig. 12 shows the packet loss rate as a function of the light intensity impinging on the solar cell. For very low light intensity, there is not enough voltage change to trigger the wake-up mechanism and the communication is affected by a high packet loss. However, this occurs at very low light level (in the order of 100 Lux), much smaller than typical suggested indoor illumination (≈ 500 Lux).

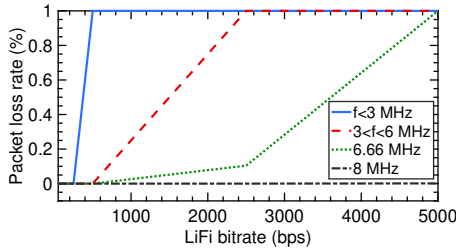


Figure 14: Baseband processing ability with LiFi bit rate. Packet loss rate increases at lower MCU frequency (f) and higher LiFi bit rate, as the processing time is greater than the incoming symbol duration.

Another parameter affecting the data acquisition is the relation between the percentage of correctly received symbols and the LiFi communication rate, with results presented in Fig. 13. At frequencies above 150 ksymbol per second, the sensitivity of the comparator is not large enough to sense the difference between high and low symbols received with the solar cell.

5.3 LiFi Reception ability

The performance of the tag as a LiFi receiver will depend not only on the before mentioned data acquisition but also on the capacity of the tag to process the data. The latter depends on the clock frequency of the MCU. Nevertheless, as the MCU is the main source of consumption on our system, it is desired to have a clock frequency as low as possible, in order to reduce the overall consumption. We evaluate the tag under different transmission rates and different MCU clock frequencies. The frequencies selected are the ones given by the manufacturer. The results are presented in Fig. 14. Below 3.33 MHz the maximum rate at which no packet is lost is 250 bps, between 3.33 MHz and 6.66 MHz at 500 bps, 2.5 kbps at 6.66 MHz and 5 kbps at 8 MHz. At each rate, from some point on, the tag is unable to receive anymore. This is the result of the MCU taking more time to process a symbol than the symbol duration.

5.4 Energy Harvesting

The operation of our tag on the energy harvested from the ambient environment is an essential functionality for our system. In this section, we present our experiments to evaluate this ability of our system under varied energy harvesting conditions.

LiFi Transmission Rate. We explore how the LiFi transmission rate impacts the energy harvesting ability. We measure the energy harvesting time as we vary the symbol rate, which impacts the incident light intensity. Fig. 15 shows the result of the experiment. We observe that varying the symbol transmission rate does not significantly impact the energy harvesting rate when compared to an unmodulated LiFi transmission. We believe this is because the amount of energy incident on the solar cell changes negligibly with the LiFi transmission rate. The high capacitance effects of the solar cell and the harvester chip further mitigate this problem.

Light Intensity. Next, we evaluate the ability of our system to harvest energy under different light intensity conditions. The incident light levels impact the energy available to harvest impacting the harvesting time. In this experiment, we explore the time taken to charge a capacitor of size 2.2 mF as we change the light intensity

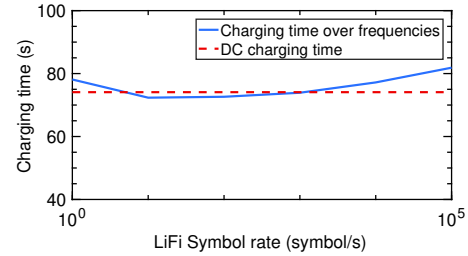


Figure 15: Capacitor charging time with LiFi symbol rate. Increasing the LiFi symbol rate does not cause appreciable increase in the energy harvesting rate when compared to harvesting energy from a un modulated light (DC signal).

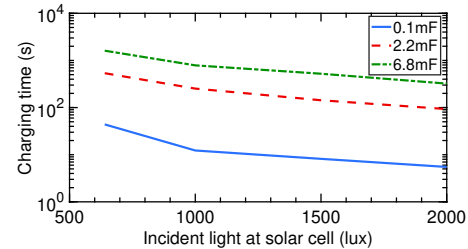


Figure 16: Charging time with capacitor sizes. We find that the energy harvesting time increases with the capacitor size.

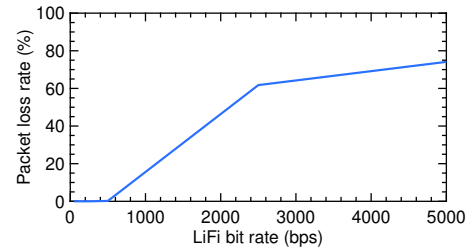


Figure 17: Packet loss rate. Due to the intermittent behavior of the tag, the packet loss rate increases with the LiFi bit rate.

levels. As shown in Fig. 16, the charging time decreases significantly with the increase in the light intensity levels.

Capacitor Size. In this experiment, we evaluate the impact of capacitor size on the energy harvesting time. A larger capacitor size can sustain the operation of the tag for a longer time duration but also takes a much longer time to charge. We experiment with similar conditions as the last experiment. We evaluate three different capacitor sizes, 100 μ F, 2.2 mF and 6.8 mF. Fig. 16 shows the results of the experiment. As expected, a small capacitor or brighter light conditions result in faster charging time. We also note that, even under normal indoor illumination, we can harvest sufficient energy to sustain the operation of our tag during reception for a few minutes with the biggest capacitor.

LiFi Reception. We evaluate the ability of our system to receive LiFi transmissions under the harvested modulated light. We configure the LiFi transmitter to transmit at different bit rates. We set the MCU at the lowest clock frequency for each transmission rate. Fig. 17 shows the result of the experiment. We observe that under such conditions, our system can continuously receive data up to 250 bps without intermittent behavior commonly shown by battery-free systems. As we increase the LiFi transmission rate, the energy harvested and used becomes asymmetric impacting the reception ability, as the tag starts to lose energy during the reception.

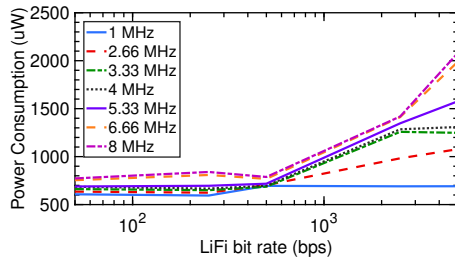


Figure 18: Power consumption and LiFi bit rate. Higher MCU clock rate are required to support base band processing at higher LiFi bit rates. We require the MCU to operate at 8 MHz to support LiFi bit rate of 5 kbps, while consuming 2 mW.

5.5 Power Consumption

In this experiment, we measure the power consumption of the tag. Two main contributors influence the power consumption of the tag: the MCU; and the consumption of the other units of the circuit. Its operating state influences the power consumption of MCU itself. We measure the power consumption using a highly sensitive Keysight E36313A power supply [28].

First, we measure the power consumption of the tag with the MCU in the lowest power state, and find that it consumes a peak power of $224\mu W$, independent from the MCU’s clock rate (as it is turned off in low power mode). This consumption is due to all the units, such as, backscatter modulator and LiFi receiver, being active.

Next, when receiving and processing LiFi data, the power consumption of the tag scales with the symbol rate and clock frequency. The amount of processing required is fixed per symbol. This means that the higher the transmission rate, the more processing MCU needs to perform, which increases the power consumption. We illustrate these results in Fig. 18. As we increase the LiFi bit rate, we need higher MCU frequency to be able to process symbols fast enough before the next symbol is received. Further, a higher transmission rate also prevents MCU from transiting to a low-power state, which also pushes the power consumption. We can achieve communication of 250 bps at $620\mu W$ by setting the MCU frequency at 1 MHz and 5 kbps at 2 mW when the MCU frequency is 8 MHz (lower clock rates would result in packet losses because of our energy-efficient LiFi reception, see Section 4.1).

5.6 LiFi as Oscillator

In this experiment, we evaluate the ability of LiFi transmitter to eliminate onboard oscillators and support frequency shift backscatter with the objective of significantly help to lower the power consumption of the tag.

We program the LiFi transmitter to generate an unmodulated carrier signal up to the frequency of 90 kHz (corresponding to 180 ksymbol/sec), which is the maximum frequency up to which we see a noticeable voltage swing across solar cell output to enable digitization operation (cf. Section 3.3.1). Next, we connect the output of the digitization mechanism to the backscatter modulator. Thus, the overall power consumption is dictated by the comparator, which results in approximately $20\mu W$. We generate a carrier signal with a strength of 17 dBm located several meters away. We locate an RF spectrum analyzer close to our battery-free tag. We keep track of the noise floor and the backscattered signal strength as we change the frequency of unmodulated carrier transmitted from LiFi emitter.

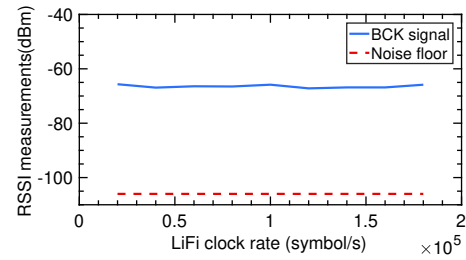


Figure 19: LiFi as Oscillator. Modulating light with a signal of frequency required for frequency shift backscatter (BCK) transmissions helps us to eliminate on board oscillators.

Fig. 19 shows the Received Signal Strength Indicator (RSSI) as a function of LiFi clock rate. For comparison, we measure the noise floor by finding the minimum level of the signal analyzer at the frequency band of 868 MHz. As we change the clock frequency of the LiFi transmitter, we observe a high backscattered signal strength which implies we can support frequency shift backscatter without requiring onboard oscillators.

5.7 Communication Range

In this experiment, we evaluate the communication range of our system. Due to the hybrid design, the communication range includes light based downlink communication, and uplink through backscatter mechanism.

LiFi Downlink. The range of the LiFi downlink system depends mainly on the intensity of the light and the sensitivity of the LiFi receiver. Our system can communicate with light intensity as small as 100 Lux. We use a 4.3 W LED in the transmitter that allows communication distance of up to 3 meters.

A low-power envelope detector has a sensitivity of around -30 dBm, as we discussed in Section 2.2. As we discussed earlier, RF signals suffer from many unintended effects and also make dense deployment challenging.

Backscatter Uplink. In the case of the backscattering communication, the communication distance depends on the relative distance between the carrier generator and tag, tag and receiver in the LED bulb, and carrier generator’s intensity. To measure the capabilities of our system as a backscatter under real deployment conditions, we place the tag in the same room as the receiver, and place the carrier generator at different locations. The sensitivity of the RF receiver in the LED bulb is around -110 dBm. The kitchen, corridor 1, room 1, room 2 and corridor 2 are located at a distance of 6, 4.5, 8.5, 15 and 20 meters, respectively, and we collect the RSSI measurements of the received packets. The kitchen has direct Line-of-Sight (LOS) with the room where the tag is located. The rest of the measurements are taken in the corridor with no LOS with the tag or in offices in the same corridor.

At each measurement point, we take measurements for 1 minute. The results of this experiment are shown in Fig. 20. The further we are from the tag the smaller the RSSI is. Nevertheless, here we show that our system can communicate at tens of meters even when objects such as walls are blocking the direct LOS of the system.

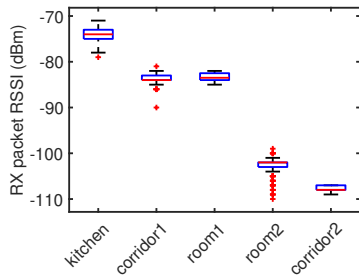


Figure 20: Received signal measurement. Backscatter signal strength for varied location of the carrier generator.

	EDISON	RetroVLC	PassiveVLC
Power Consumption Downlink Frontend (μ W)	20	N/A	N/A
Power Consumption Uplink Frontend (μ W)	70 (2.9 kbps)	90 (0.5 kbps)	90 (0.5 kbps)
Uplink rate (kbps)	2.9	0.125	1
Downlink distance per LED consumption (m/W)	0.7	0.16	N/A
max. uplink distance (m)	>20	2.4	4.5
Non-disturbing uplink light for user	Yes	No	No
Suffers from directionality	No	Yes	Yes

Table 3: Comparison of EDISON with battery-free works using LiFi both for downlink and uplink. For fairness, we use LEDs as transmitters in all cases (PassiveVLC did not report the results with LEDs but only with flash lights). These systems use one of the variant of MSP430 MCU. For the variant we use we have optimized it to consume $\approx 200 \mu$ W operating at 1 MHz. Because of the MCU, all these systems may achieve similar downlink rate under sufficient power budget.

5.8 Comparison with RF/LiFi systems

To better understand the benefits of our solution, we emphasize the advantages of using it versus single technology solutions.

LiFi systems. Uplink capability restricts battery-free LiFi systems. Recent systems have leveraged VLC backscatter mechanisms to support uplink transmissions [29, 64], using retro reflectors to backscatter and modulate incident light. We compare EDISON to these systems in Table 3. EDISON supports a significantly higher range, bit rate, and does not suffer from directional issues. Comparing the energy cost for performing up link transmissions, EDISON uses RF backscatter mechanism based on LoRea [57], and consumes 70μ W at an rate of 2.9 kbps. LoRea demonstrates significantly higher bitrates with similar modulator design, which may enable us to increase this rate without incurring additional energy [57]. We find that retro reflectors based VLC backscatter systems consume higher power, and are restricted due to slow switching speed (approx. 1 KHz) and high peak power consumption of the LCD screen. RetroVLC consumes approx. 90μ W at a switching rate of 0.5 KHz. PassiveVLC [64] would consume similar power, as it also based on circuit designs of RetroVLC [29].

RF backscatter systems. We find that EDISON LiFi frontend and RF envelope detector consume similar energy for reception. This is because the only active and energy-consuming component in both these systems is a comparator. However, RF envelope detector is limited by the challenges introduced in Section 2.2, that largely increase the energy consumption of the MCU in real setting at a reduced power budget.

6 RELATED WORK

Our system is related to works that devise mechanisms to support passive communication and their applications.

Applications of passive communication. There is a growing number of applications that have been recently investigated for passive communication, that use backscatter or visible light as a communication medium. These applications include a battery-free eye-tracker for augmented reality [30], wristband for hand gesture recognition [56], the first phone to make calls without batteries [48], and battery-free cameras and HD video streaming [37, 38]. However, all these works share the limitations that devices mainly transmit data, or the reception of data at the device is at very low rate or constrained. Further they face challenges such as those we mentioned in the Section 2.

Network densification. Networks are getting more densely deployed to increase capacity and reduce latency, rather than for communicating to battery-free devices. The underlying radio technologies, mm-wave and Massive MIMO, are power-hungry and use high frequencies to optimize the spectrum reuse [21, 25]. There has been work to make battery-free devices talking to current architectures and exploiting existing RF waves [9, 26, 34, 43], rather than relying on isolated, costly and low-performance deployments of RFID readers. However, all these works are affected by fundamental limitations, such as (i) they can not scavenge enough RF energy as legacy transmissions are typically wideband, while peak power of energy harvested occurs for narrowband transmissions; (ii) they all work only for uplink communication from the battery-free device.

Receptions on low-power visible light systems. In the last years, we have seen an increasing interest in energy-efficient designs for VLC and Visible Light Sensing systems. They optimize the sensing circuitry and processing logic for energy-efficient operations. [32] operates photodiodes in a photovoltaic mode, which eliminates the need for energy-expensive trans-impedance amplifiers. They detect slow changes in the light conditions to design a self-powered hand gesture detection system. [36, 59] leverage solar cells instead of photodiodes for detecting changes in the light conditions caused due to the hand gestures. However, [32, 36] used an energy-expensive ADCs for digitization, and further, all of these systems detect slow changes (few tens of Hz) caused due to gestures. Solar cells have also been used to support high-speed LiFi communication [63]. However, such systems use energy-expensive mechanisms (ADCs, Oscilloscope) and are infeasible for low-power systems such as those we target that operate on harvested energy.

Overheads of high rate sampling using an energy-expensive ADCs are prominent for LiFi systems. Consequently, recent systems eliminate ADCs using an energy inexpensive thresholding circuits. RetroVLC [29] and PassiveVLC [64] use a thresholding circuit to digitize light readings. However, these systems use an energy-expensive photodiode coupled with an amplifier, we overcome this using a solar cell. Further, to overcome the overhead of energy-expensive digitization, we combine the solar cell with the shareholding circuit. As compared to [59] who used such a design of gesture sensing, we demonstrate the ability to receive LiFi transmission. Further, we also tackle the challenges of energy-efficient and necessary baseband processing.

Passive VLC Uplink. Another body of work has explored passive uplink communication for VLC where the receiver replies using an LCD shutter to change the reflected signal in time and sends

the signal in the direction of the transmitter (LED) using a retro-reflector [29, 64]. An alternative scheme proposed in [10] uses the mobility and the reflective properties of materials to send data to the receive. Table 3 we provide a comparison between our system and these related systems. We overcome their limitations through the use of RF backscatter to support uplink transmissions.

Intersection of different technologies. There has been limited investigation on the study of the interface between different technologies. A low-power transceiver called Morpho was presented in [45] to integrate active radio components with passive radio components. Similar interest has emerged to understand the interaction between radio and acoustic [55]. Yet, these works do not operate in battery-free regime. There has also been limited research to integrate visible light and radio-based communication. [39, 62] did not consider battery-free devices and purely aimed at optimizing the throughput. Related work has investigated how to sense coarse light variations in order to modulate the RF backscatter signal [59]. The proposed solution did not allow to send data to the IoT tag. [19] proposed to retrofit LEDs with an RFID reader to communicate to battery-free device. Their design is cost prohibitive (\approx \$300) and subjected to low sensitivity and high transmit power beyond regulatory compliance. This paper is inspired by our preliminary work [17], where an RF carrier generator is integrated in each LED bulb. This increases the complexity in coordinating RF emitters.

7 DISCUSSION

We discuss potential improvements in our design, scalability issues and application scenarios enabled by our system.

7.1 Role of LiFi and RF in Deployments

Our system only uses RF backscatter for uplink transmissions. However, it can either use light or RF signals for receptions and energy harvesting. The usage of these mediums depends on the application scenario and deployment conditions. For most scenarios, as we had discussed earlier, indoor light is homogeneous in space, and EDISON uses light as a medium. But RF energy is more homogeneous in time, while the ambient light could be unavailable or low depending on the time of the day and night. Under low ambient light EDISON may solely use RF envelope detector for harvesting and reception. We might also prefer to use a RF envelope detector over light when operating in proximity to edge device where the carrier signal might be stronger. Moreover, our design could use RF and light to harvest, as demonstrated in [46].

7.2 Scaling deployment

We have presented the design of our system and micro-benchmarked the performance of a single tag. We can support a large number of tags with little or no modification. The scalability of our system depends on the uplink, downlink, harvesting ability and cost per device. We had seen that the light levels indoors are uniform through space (harvesting and link quality). We can identify individual tags using the address field in the frame structure as presented in Table 1 from a single LED. We can use this together with our wake-up mechanism to trigger the desired tag. The uplink ability depends on the RF-backscatter mechanism. Recent systems have demonstrated a large number of concurrently backscatter tags [22].

We implement the RF-uplink similarly to LoRea [57]. Its frequency division multiplexing (FDM) mechanisms was presented in [58], reusable in our design. RF backscatter signals are received by our LED bulbs. In our case, we receive a FSK modulated signal received using a commodity radio transceiver. Such a transceiver can be easily integrated in existing LED bulbs. In addition, the upcoming 802.11bb Light Communication [1] (completed in 2021) addresses mass market requirements for LiFi, and will allow a single chipset with 802.11bb to transmit and receive with light and RF.

7.3 Application Scenarios

We find that many deployments offer favorable conditions for our system. We list some of these in this section.

Sensors in homes. Sensors deployed in home enable scenarios such as occupancy detection. Consequently, their energy-efficient operation has attracted interest, and backscatter has emerged as a promising technology. However, such a possibility is restricted due to challenges such as those we discussed in Section 2. Homes provide necessary conditions for our system. The lighting infrastructure is pervasive, and commonly provides homogeneous light levels. Further, WiFi and other router devices can function as an edge device for our system.

Greenhouses. Sensors are being increasingly used in farming applications to improve their yield [61]. However, at present deploying and maintaining sensors at a large scale is cumbersome due to overhead associated with batteries. Backscatter based sensors are attractive for these applications [24]. Greenhouses could provide the necessary conditions for our system. Greenhouses are well illuminated with controlled lighting. These lights could help us coordinate the deployment of a large number of sensors.

Outdoors. Our system could also enable outdoor sensor applications. In these applications, artificial lighting for illumination, such as street lights which are usually bright, could provide necessary LiFi downlink capability. Thanks to RF backscatter, deployments can be at a reasonable distance away from the lighting source.

8 CONCLUSION

In this paper, we have proposed a novel LiFi-RF communication system that addresses some of the fundamental roadblocks that impede the vision of battery-free communication. We envision that the ability to operate battery-free will allow to deploy a massive number of IoT devices. The system exploits the advantages of LiFi and RF to provide battery-free communication and addresses technical solutions to solve their bottlenecks. We have presented several contributions to communicate at very low power, and have shown that EDISON can allow continuous reception of LiFi data up to 250 bit/s using only energy harvested from the LiFi transmitter.

ACKNOWLEDGEMENTS

We are grateful to Deepak Ganesan for the constructive feedback. We also thank the shepherd Wenjun Hu, and the anonymous reviewers whose insightful comments and guidance have been very helpful in improving this paper. The project that gave rise to these results received the support of a fellowship from “la Caixa” Foundation (ID 100010434). The fellowship code is LCF/BQ/ES16/11570019. Further, this work has also been partly funded by the Swedish Research Council (VR, grant 2018-05480).

REFERENCES

- [1] Ieee project 802.11bb, standard for information technology telecommunications and information exchange between systems local and metropolitan area networks - specific requirements - part 11: Wireless lan medium access control (mac) and physical layer (phy) specifications amendment: Light communications.
- [2] A. Abedi, M. H. Mazaheri, O. Abari, and T. Brecht. Witag: Rethinking backscatter communication for wifi networks. In *Proceedings of the 17th ACM Workshop on Hot Topics in Networks*, HotNets '18, pages 148–154, New York, NY, USA, 2018. ACM.
- [3] Ablic. https://www.ablic.com/en/doc/datasheet/voltage_regulator/s1313_e.pdf.
- [4] Analog Devices. Hmc190bms8. <https://www.analog.com/media/en/technical-documentation/data-sheets/hmc190b.pdf>.
- [5] Analog Devices. <https://www.analog.com/media/en/technical-documentation/data-sheets/adg904.pdf>.
- [6] I. Analytics. State of the IoT 2018: Number of IoT devices now at 7B. 2018.
- [7] M. Anderson. Potential Hazards at Both Ends of the Lithium-Ion Life Cycle. *IEEE Spectrum*, 2013.
- [8] BeagleBoard. https://cdn-shop.adafruit.com/datasheets/bbb_srm.pdf.
- [9] D. Bharadia, K. R. Joshi, M. Kotaru, and S. Katti. Backfi: High throughput wifi backscatter. *SIGCOMM Comput. Commun. Rev.*, 45(4), Aug. 2015.
- [10] R. Bloom, M. Zuniga, Q. Wang, and D. Giustiniano. Tweeting with sunlight: Encoding data on mobile objects. In *IEEE INFOCOM*, 2019.
- [11] Broadcom Limited. Hsms286c. <https://www.digikay.com/product-detail/en/broadcom-limited/hsms-286c-trig/516-1822-1-nd/1966528>.
- [12] A. Colin, E. Ruppel, and B. Lucia. A reconfigurable energy storage architecture for energy-harvesting devices. In *Proceedings of the Twenty-Third International Conference on Architectural Support for Programming Languages and Operating Systems*, pages 767–781, 2018.
- [13] Ettus Research. https://www.ettus.com/wp-content/uploads/2019/01/b200-b210_spec_sheet.pdf.
- [14] E. C. for Standardization. Light and Lighting-Lighting of work places-Part 1: Indoor work places. *European Std. EN 12 464-1*, June 2011.
- [15] A. Galisteo, D. Juara, and D. Giustiniano. Research in visible light communication systems with openv1c1.3. In *5th IEEE World Forum on Internet of Things, WF-IoT 2019, Limerick, Ireland, April 15-18, 2019*, pages 539–544, 2019.
- [16] A. Galisteo, H. Wu, Q. Wang, D. Juara, M. Zuniga, and D. Giustiniano. Openv1c1.2 for increased data rate with embedded systems. In *Proceedings of the 4th ACM Workshop on Visible Light Communication Systems*, pages 33–33. ACM, 2017.
- [17] D. Giustiniano, A. Varshney, and T. Voigt. Connecting battery-free iot tags using led bulbs. In *Proceedings of the 17th ACM Workshop on Hot Topics in Networks*, HotNets '18, pages 99–105, New York, NY, USA, 2018. ACM.
- [18] J. Gummeson, S. S. Clark, K. Fu, and D. Ganesan. On the limits of effective hybrid micro-energy harvesting on mobile crfd sensors. In *Proceedings of the 8th International Conference on Mobile Systems, Applications, and Services*, MobiSys '10, page 195–208, New York, NY, USA, 2010. Association for Computing Machinery.
- [19] J. Gummeson, J. Mccann, C. Yang, D. Ranasinghe, S. Hudson, and A. Sample. Rfid light bulb: Enabling ubiquitous deployment of interactive rfid systems. *Proc. ACM Interact. Mob. Wearable Ubiquitous Technol.*, 1(2), June 2017.
- [20] H. Haas. High-speed wireless networking using visible light. *SPIE Newsroom*, 1(1), 2013.
- [21] S. Han, C. I. I. Z. Xu, and C. Rowell. Large-scale antenna systems with hybrid analog and digital beamforming for millimeter wave 5g. *IEEE Communications Magazine*, 53(1), January 2015.
- [22] M. Hesar, A. Najafi, and S. Gollakota. Netscatter: Enabling large-scale backscatter networks. In *Proceedings of the 16th USENIX Conference on Networked Systems Design and Implementation*, NSDI'19, page 271–283, USA, 2019. USENIX Association.
- [23] IXYS. Slmd121h04l. <http://ixapps.ixys.com/datasheet/slmd121h04l-data-sheet.pdf>.
- [24] C. Josephson, B. Barnhart, S. Katti, K. Winstein, and R. Chandra. Rf soil moisture sensing via radar backscatter tags, 2019.
- [25] M. Kamel, W. Hamouda, and A. Youssef. Ultra-dense networks: A survey. *IEEE Communications Surveys Tutorials*, 18(4), Fourthquarter 2016.
- [26] B. Kellogg, A. Parks, S. Gollakota, J. Smith, and D. Wetherall. Wi-Fi backscatter: Internet connectivity for RF-powered devices. In *ACM SIGCOMM*, 2014.
- [27] B. Kellogg, V. Talla, S. Gollakota, and J. R. Smith. Passive wi-fi: Bringing low power to wi-fi transmissions. In *Proceedings of the 13th Usenix Conference on Networked Systems Design and Implementation*, NSDI'16, pages 151–164, Berkeley, CA, USA, 2016. USENIX Association.
- [28] Keysight. DC Programmable Power Supply E36313A. <https://literature.cdn.keysight.com/litweb/pdf/E36311-90001.pdf>, 2019.
- [29] J. Li, A. Liu, G. Shen, L. Li, C. Sun, and F. Zhao. Retro-vlc: enabling battery-free duplex visible light communication for mobile and iot applications. In *Proceedings of the 16th International Workshop on Mobile Computing Systems and Applications*, pages 21–26. ACM, 2015.
- [30] T. Li and X. Zhou. Battery-free eye tracker on glasses. In *ACM MobiCom '18*, New York, NY, USA, 2018.
- [31] X. Li, B. Hussain, L. Wang, J. Jiang, and C. P. Yue. Design of a 2.2-mw 24-mb/s cmos vlc receiver soc with ambient light rejection and post-equalization for li-fi applications. *Journal of Lightwave Technology*, 36(12):2366–2375, June 2018.
- [32] Y. Li, T. Li, R. A. Patel, X.-D. Yang, and X. Zhou. Self-powered gesture recognition with ambient light. In *Proceedings of the 31st Annual ACM Symposium on User Interface Software and Technology*, pages 595–608, 2018.
- [33] Linear Technology. <https://www.analog.com/media/en/technical-documentation/data-sheets/6906fc.pdf>.
- [34] V. Liu, A. Parks, V. Talla, S. Gollakota, D. Wetherall, and J. R. Smith. Ambient backscatter: Wireless communication out of thin air. In *Proceedings of the ACM SIGCOMM 2013 Conference on SIGCOMM*, SIGCOMM '13, pages 39–50, New York, NY, USA, 2013. ACM.
- [35] B. Lucia, V. Balaji, A. Colin, K. Maeng, and E. Ruppel. Intermittent computing: Challenges and opportunities. In *2nd Summit on Advances in Programming Languages (SNAPL 2017)*. Schloss Dagstuhl-Leibniz-Zentrum fuer Informatik, 2017.
- [36] D. Ma, G. Lan, M. Hassan, W. Hu, M. B. Upama, A. Uddin, and M. Youssef. Solargest: Ubiquitous and battery-free gesture recognition using solar cells. In *The 25th Annual International Conference on Mobile Computing and Networking*, MobiCom '19, New York, NY, USA, 2019. Association for Computing Machinery.
- [37] S. Naderiparizi, M. Hesar, V. Talla, S. Gollakota, and J. R. Smith. Towards battery-free HD video streaming. In *NSDI 18*. USENIX, 2018.
- [38] S. Naderiparizi, A. N. Parks, Z. Kapetanovic, B. Ransford, and J. R. Smith. Wispcam: A battery-free rfid camera. In *2015 IEEE International Conference on RFID (RFID)*, pages 166–173. IEEE, 2015.
- [39] S. Naribole, S. Chen, E. Heng, and E. W. Knightly. Lira: A wlan architecture for visible light communication with a wi-fi uplink. *IEEE SECON*, 2017.
- [40] A. Nordrum. The Internet of Fewer Things. *IEEE Spectrum*, 2016.
- [41] On Semiconductor. <https://www.onsemi.com/pub/collateral/ncs2200-d.pdf>.
- [42] PowerFilm. MP3-37.
- [43] S. P. Y. F. X. T. H. Y. X. W. Renjie Zhao, Fengyuan Zhu. Ofdma-enabled wi-fi backscatter. In *ACM MobiCom '19*, 2019.
- [44] M. Rostami, J. Gummeson, A. Kiaghadi, and D. Ganesan. Polymorphic radios: A new design paradigm for ultra-low power communication. In *Proceedings of the 2018 Conference of the ACM Special Interest Group on Data Communication*, SIGCOMM '18, pages 446–460, New York, NY, USA, 2018. ACM.
- [45] M. Rostami, J. Gummeson, A. Kiaghadi, and D. Ganesan. Polymorphic radios: A new design paradigm for ultra-low power communication. In *ACM SIGCOMM '18*, New York, NY, USA, 2018.
- [46] A. Saffari, M. Hesar, S. Naderiparizi, and J. R. Smith. Battery-free wireless video streaming camera system. In *2019 IEEE International Conference on RFID (RFID)*, pages 1–8, 2019.
- [47] V. Talla, M. Hesar, B. Kellogg, A. Najafi, J. R. Smith, and S. Gollakota. Lora backscatter: Enabling the vision of ubiquitous connectivity. *Proc. ACM Interact. Mob. Wearable Ubiquitous Technol.*, 1(3):105:1–105:24, Sept. 2017.
- [48] V. Talla, B. Kellogg, S. Gollakota, and J. R. Smith. Battery-free cellphone. *IMWUT*, 1(2), 2017.
- [49] V. Talla, B. Kellogg, B. Ransford, S. Naderiparizi, S. Gollakota, and J. R. Smith. Powering the next billion devices with wi-fi. In *Proceedings of the 11th ACM Conference on Emerging Networking Experiments and Technologies*, pages 1–13, 2015.
- [50] M. M. Tentzeris, A. Georgiadis, and L. Roselli. Energy harvesting and scavenging. *Proc. IEEE*, 102(11), 2014.
- [51] Texas Instruments. <http://www.ti.com/lit/ds/symlink/cc1310.pdf>.
- [52] Texas Instruments. MSP430FR5949. <http://www.ti.com/lit/ds/symlink/msp430fr5949.pdf>.
- [53] Texas Instruments. bq25570. <http://www.ti.com/lit/ds/symlink/bq25570.pdf>.
- [54] Z. Tian, K. Wright, and X. Zhou. The darklight rises: Visible light communication in the dark: Demo. In *Proceedings of the 22Nd Annual International Conference on Mobile Computing and Networking*, MobiCom '16, pages 495–496, New York, NY, USA, 2016. ACM.
- [55] F. Tonolini and F. Adib. Networking across boundaries: Enabling wireless communication through the water-air interface. In *ACM SIGCOMM '18*, New York, NY, USA, 2018.
- [56] H. Truong, S. Zhang, U. Muncuk, P. Nguyen, N. Bui, A. Nguyen, Q. Lv, K. Chowdhury, T. Dinh, and T. Vu. Capband: Battery-free successive capacitance sensing wristband for hand gesture recognition. In *ACM SenSys '18*, New York, NY, USA, 2018.
- [57] A. Varshney, O. Harms, C. Pérez-Penichet, C. Rohner, F. Hermans, and T. Voigt. Lorea: A backscatter architecture that achieves a long communication range. In *Proceedings of the 15th ACM Conference on Embedded Network Sensor Systems*, SenSys '17, pages 18:1–18:14, New York, NY, USA, 2017. ACM.
- [58] A. Varshney, C. P. Penichet, C. Rohner, and T. Voigt. Towards wide-area backscatter networks. In *Proceedings of the 4th ACM Workshop on Hot Topics in Wireless*, HotWireless '17, pages 49–53, New York, NY, USA, 2017. ACM.
- [59] A. Varshney, A. Soleiman, L. Mottola, and T. Voigt. Battery-free visible light sensing. In *Proceedings of the 4th ACM Workshop on Visible Light Communication Systems*, VLCS '17, pages 3–8, New York, NY, USA, 2017. ACM.

- [60] A. Varshney, A. Soleiman, and T. Voigt. Tunnelscatter: Low power communication for sensor tags using tunnel diodes. In *The 25th Annual International Conference on Mobile Computing and Networking*, MobiCom '19, pages 50:1–50:17, New York, NY, USA, 2019. ACM.
- [61] D. Vasisht, Z. Kapetanovic, J. Won, X. Jin, R. Chandra, S. Sinha, A. Kapoor, M. Sudarshan, and S. Stratman. Farmbeats: An iot platform for data-driven agriculture. In *14th {USENIX} Symposium on Networked Systems Design and Implementation ({NSDI} 17)*, pages 515–529, 2017.
- [62] Y. Wang, D. A. Basnayaka, X. Wu, and H. Haas. Optimization of load balancing in hybrid lifi/rrf networks. *IEEE Transactions on Communications*, 65(4), April 2017.
- [63] Z. Wang, D. Tsonev, S. Videv, and H. Haas. On the design of a solar-panel receiver for optical wireless communications with simultaneous energy harvesting. *IEEE Journal on Selected Areas in Communications*, 33(8):1612–1623, 2015.
- [64] X. Xu, Y. Shen, J. Yang, C. Xu, G. Shen, G. Chen, and Y. Ni. Passivevlc: Enabling practical visible light backscatter communication for battery-free iot applications. In *Proceedings of the 23rd Annual International Conference on Mobile Computing and Networking*, MobiCom '17, pages 180–192, New York, NY, USA, 2017. ACM.
- [65] P. ZHANG, M. Rostami, P. Hu, and D. Ganesan. Enabling practical backscatter communication for on-body sensors. In *Proceedings of the 2016 ACM SIGCOMM Conference*, SIGCOMM '16, pages 370–383, New York, NY, USA, 2016. ACM.